ELSEVIER

Journal of Organometallic Chemistry 630 (2001) 205–214

Journal of Organometallic Chemistry

www.elsevier.com/locate/jorganchem

# Synthesis, crystal structures and spectroscopic studies of diorganotin derivatives with mefenamic acid. Crystal and molecular structures of 1,2:3,4-di-$\mu_2$-2-[(2,3-dimethylphenyl)amino]-benzoato-*O*,*O*-1,3-bis-2-[(-[(2,3-dimethylphenyl)amino]benzoato-*O*-1,2,4:2,3,4-di-$\mu_3$-oxo-tetrakis[di-methyltin(IV)] and 1,2:3,4-di-$\mu_2$-2-[(-[(-[(2,3-dimethylphenyl)amino]-benzoato-*O*,*O*-1,3-bis-2-[(-[(-[(2,3-dimethylphenyl)amino]benzoato-*O*-1,2,4:2,3,4-di-$\mu_3$-oxo-tetrakis[di-*n*-butyltin(IV)]

Vaso Dokorou [a], Zbigniew Ciunik [b], Umberto Russo [c], Dimitra Kovala-Demertzi [a,*]

[a] *Inorganic Chemistry, Department of Chemistry, University of Ioannina, 45110 Ioannina, Greece*
[b] *Faculty of Chemistry, University of Wrocław, 14 F. Joliot-Curie St., 50-383 Wrocław, Poland*
[c] *Dipartimento di Chimica Inorganica, Metallorganica e Analitica, Università di Padova, Via Loredan 4, I-35131 Padua, Italy*

Received 9 March 2001; received in revised form 31 May 2001; accepted 31 May 2001

**Abstract**

The complexes $[Me_2LSnOSnLMe_2]_2$ (**1**) and $[Bu_2LSnOSnLBu_2]_2$ (**2**) where HL is 2-[(2,3-dimethylphenyl)amino]benzoic acid (mefenamic acid), have been prepared and structurally characterized by means of $^{119}$Sn Mössbauer, vibrational and NMR ($^1$H and $^{13}$C) spectroscopies. The crystal structures of complexes **1** and **2** have been determined by X-ray crystallography. Each structure is centro-symmetric and features a central rhombus $Sn_2O_2$ unit with two additional tin atoms linked at the O atoms. Pairs of tin atoms are bridged by bidentate carboxylate ligands and the 'external' tin atoms have their coordination geometry completed by a bridging bidentate carboxylate ligand for **1** and by a monodentate carboxylate ligand for **2**. Five rings, each containing two tin atoms, are present in the dimeric tetraorganodistannoxane **1** and the geometry around the four tin centers is distorted octahedral for Sn(2) and Sn(2a) and trigonal bipyramidal for Sn(1) and Sn(1a). Three such rings are present in **2** and the geometry around the four five-coordinated tin centers, Sn(1), Sn(1a), Sn(2) and Sn(2a), is distorted square-bipyramidal. Significant $\pi \rightarrow \pi$, C–H $\rightarrow \pi$ stacking interactions and intramolecular hydrogen bonds stabilize structures **1** and **2**. The polar imino hydrogen atom participates in intramolecular hydrogen bonds. Complexes **1** and **2** are self-assembled via $\pi \rightarrow \pi$, C–H $\rightarrow \pi$ and stacking interactions. 

*Keywords:* Mefenamic acid; Diorganotin; Crystal structures; Spectroscopic studies

## 1. Introduction

Mefenamic acid (i.e. 2-[(2,3-dimethylphenyl)-amino]benzoic acid or *N*-(2,3-xylyl)anthranilic acid), structure 1, belongs to a family of non-steroidal anti-inflammatory drugs (NSAIDs) that are derivatives of *N*-phenylanthranilic acid. NSAIDs are among the most frequently used medicinal drugs. They are utilized primarily as analgesics, anti-inflammatories and antipyretics and their side effects have been well studied. The therapeutic activity of these analgesics is believed to be due to their ability to inhibit the biosynthesis of prostaglandins by competitive interaction with the cyclooxygenase–arachidonic acid complex or by radical-quenching agents that interfere with the initiation of the

* Corresponding author. Fax: +30-651-44825.
*E-mail address:* dkovala@cc.uoi.gr (D. Kovala-Demertzi).

0022-328X/01/$ - see front matter 
PII: S0022-328X(01)01026-9

cyclooxygenase reaction [1]. Several NSAIDs have been used in combination with cytotoxic drugs, and the interactions of mefenamic acid, sulindac and indomethacin with cyclophosphamide, melphalanor carmustine have been studied [2]. A specific group of NSAIDs, indomethacin, sulindac, tolmetin, acemetacin, zomepirac and mefenamic, all at non-toxic levels, significantly increased the cytotoxicity of the anthracyclines, doxorubicin, daunorubicin and epirubicin, as well as teniposide, VP-16 and vincristine [3]. Mefenamic acid chemically resembles tolfenamic [4] and flufenamic acids and other fenamates in clinical use. Complexes of mefenamic acid with iron(III) [5a], sodium(I) and calcium(II) [5] have been reported. Characterization of the complexes based on spectroscopic results was performed and possible structures were proposed [5]. The crystal structures of mefenamic acid and of a copper(II) complex have been solved [6].

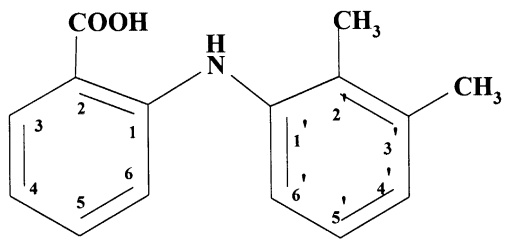

(1)

Organotin(IV) carboxylates form an important class of compound and have received increasing attention in recent years, not only because of their intrinsic interest but also owing to their varied applications. These compounds find wide use as catalysts and stabilizers, and certain derivatives are used as biocides, as antifouling agents and as wood preservatives [7]. Investigations have been carried out to test their anti-tumor activity and it has been observed that indeed several di- and triorganotin species show potentiality as antineoplastic agents [8].

Given the pharmacological importance of mefenamic acid and the potential biological activity of organotin carboxylates, it was thought of some interest to explore the chemistry of organotin/mefenamic acid compounds. As a continuation of our studies of biological organotin chemistry [9] and on the coordination chemistry and anti-inflammatory properties of NSAIDs such as diclofenac and tolfenamic acids [4,10], we report here the synthesis and spectral characterization of $[R_2LSnOSnLR_2]_2$ (where $R = CH_3$ (**1**), Bu (**2**) and L is deprotonated mefenamic acid). The complexes have been structurally characterized in the solid state by means of $^{119}$Sn Mössbauer and vibrational spectroscopy and in solution by $^1$H- and $^{13}$C-NMR spectroscopic studies. The crystal and molecular structures of **1** and **2** are also described, these being the first structures of organometallic mefenamic acid derivatives to be reported.

## 2. Experimental

### 2.1. General and instrumental

The reagents (Aldrich, Merck) were used as supplied while the solvents were purified according to standard procedures. Mefenamic acid was a gift from 'VIANNEX A.E.'. C, H, and N analyses were carried out by the microanalytical service of the University of Ioannina. Melting points were determined in open capillaries and are uncorrected. Infrared and far-infrared spectra were recorded on a Nicolet 55XC Fourier transform spectrophotometer using KBr pellets (4000–400 $cm^{-1}$) and Nujol mulls dispersed between polyethylene disks (400–40 $cm^{-1}$). The $^1$H (250.13 MHz), and $^{13}$C (62.90 MHz) NMR specta were recorded on a Bruker AC-250 spectrometer. Samples were dissolved in $CDCl_3$ or DMSO-$d_6$ and spectra were obtained at room temperature (r.t.) with the signal of the free DMSO or $CHCl_3$ (at 2.49 and 7.24 ppm, respectively) as a reference. Cross-peaking of heteronuclear multiple quantum correlation (HMQC) and heteronuclear multiple bond correlation (HMBC) gradient-assisted spectra of mefenamic acid were performed. Mössbauer spectra were recorded on finely ground materials at 80.0 K using an Air Liquid cryostat. The $Ca^{119}SnO_3$ source (15 mCi New England Nuclear) at room temperature (r.t.) was moved in a constant acceleration mode with a triangular wave form. Suitable computer programs were employed in the fitting procedure of the experimental spectra to Lorentzian line shapes. The estimated errors on the Mössbauer parameters are $\pm 0.01$ mm $s^{-1}$.

### 2.2. Synthesis

#### 2.2.1. $[Me_2LSnOSnLMe_2]_2$ (1)

A solution of mefenamic acid (0.262 g, 1 mmol) was added to a solution of dimethyl tin oxide (0.198 g, 1.15 mmol) in benzene (40 ml). The reaction mixture was refluxed for 24 h with azeotropic removal of water via a Dean–Stark trap. The resulting clear yellow solution was rotary evaporated under vacuum to a small volume, chilled and triturated with *n*-pentane to give a yellow solid. The solid was filtered off, washed with $Et_2O$ and dried in vacuo over silica gel; m.p. 183–184 °C; yield 65%. Anal. Found: C, 51.59; H, 5.11; N, 3.26. Calc.: C, 51.42; H, 5.04; N, 3.52%.

#### 2.2.2. $[Bu_2LSnOSnLBu_2]_2$ (2)

Di-*n*-butyl tin oxide (0.286 g, 1.15 mmol) and mefenamic acid (0.241 g, 1.00 mmol) were refluxed in 40 ml benzene for 24 h with azeotropic removal of water via a Dean–Stark trap. The resulting clear solution was rotary evaporated under vacuum to a small volume. Drops of *n*-pentane were added and after slow evaporation, a yellow powder was isolated; m.p. 115–117 °C;

yield 53%. Anal. Found: C, 57.95; H, 6.80; N, 2.76. Calc.: C, 57.45; H, 6.65; N, 2.91%.

### 2.3. X-ray crystallography

Crystal data are given in Table 1, together with refinement details. All measurements of crystals were performed on a Kuma KM4CCD kappa-axis diffractometer with graphite-monochromated Mo–$K_\alpha$ radiation. The crystals were positioned at 65 mm from the KM4CCD camera. Six hundred and twelve frames were measured at 0.75° intervals with a counting time of 30 s. The data were corrected for Lorentz and polarization effects. No absorption correction was applied. Data reduction and analysis were carried out with the Kuma Diffraction (Wroclaw) programs. The structures were solved by direct methods and refined by the full-matrix least-squares method on all $F^2$ data using the SHELXL97 program [11]. Non-hydrogen atoms were refined with anisotropic thermal parameters; hydrogen atoms were included from the molecular geometry and $\Delta\rho$ maps but were not refined. For **2** one symmetry-independent butyl group is partly disordered (the C(7), C(8), C(7′), and C(8′) atoms). The occupancy parameters for the respective groups of atoms are 0.6 and 0.4.

Table 1
Crystal data and structure refinement parameters for **1** and **2**

| | **1** | **2** |
|---|---|---|
| Empirical formula | $C_{68}H_{80}N_4O_{10}Sn_4$ | $C_{92}H_{128}N_4O_{10}Sn_4$ |
| Formula weight | 1588.12 | 1924.74 |
| Temperature (K) | 100(2) | 100(2) |
| Wavelength (Å) | 0.71073 | 0.71073 |
| Crystal system | Triclinic | Triclinic |
| Space group | $P\bar{1}$ | $P\bar{1}$ |
| Unit cell dimensions | | |
| $a$ (Å) | 9.898(1) | 11.319(1) |
| $b$ (Å) | 12.009(1) | 12.115(1) |
| $c$ (Å) | 15.498(1) | 19.101(2) |
| $\alpha$ (°) | 68.14(1) | 92.29(1) |
| $\beta$ (°) | 76.52(1) | 105.34(1) |
| $\gamma$ (°) | 87.03(1) | 116.66(1) |
| Volume (Å$^3$) | 1661.4(2) | 2218.9(4) |
| $Z$ | 1 | 1 |
| $D_{calc}$ (Mg m$^{-3}$) | 1.587 | 1.440 |
| Absorption coefficient (mm$^{-1}$) | 1.545 | 1.171 |
| $F(000)$ | 796 | 988 |
| Crystal size (mm) | $0.12\times0.07\times0.07$ | $0.20\times0.20\times0.12$ |
| Diffractometer | Kuma KM4CCD | Kuma KM4CCD |
| $\theta$ range for data collection (°) | 3.40–28.76 | 3.29–28.77 |
| Index ranges | $-13\le h\le10$, $-15\le k\le15$, $-20\le l\le20$ | $-14\le h\le11$, $-16\le k\le16$, $-24\le l\le24$ |
| Reflections collected | 12 028 | 16 067 |
| Independent reflections | 7568 [$R_{int}=0.0267$] | 10 103 [$R_{int}=0.0230$] |
| Data/parameters | 7568/548 | 10 103/514 |
| Final $R$ indices [$I>2\sigma(I)$] | $R_1=0.0278$ $wR_2=0.0592$ | $R_1=0.0445$ $wR_2=0.0971$ |
| Goodness-of-fit on $F^2$ | 0.987 | 1.067 |
| Largest difference peak and hole (e Å$^{-3}$) | 1.682 and −0.778 | 2.486 and −1.384 |

## 3. Results and discussion

### 3.1. Crystal structures of **1** and **2**

Compounds **1** and **2** are obtained by azeotropic removal of water produced by the reaction between the diorganotin oxide and mefenamic acid in the molar ratio 1:1. The molecular structures of **1** and **2** are shown in Figs. 1 and 2, respectively, and selected interatomic parameters are collected in Table 2. Compounds **1** and **2** are centro-symmetric dimers built up around the planar cyclic $Sn_2O_2$ unit. The two oxygen atoms O(1) and O(1a) are triply bridging, each linking one *exo*-cyclic (Sn(1) or Sn(1a)) and two *endo*-cyclic (Sn(2) and Sn(2a)) atoms. Additional links between the *exo*- and *endo*-cyclic tin centers Sn(1) and Sn(2), respectively, are provided by four bidentate bridging carboxylate ligands for **1**, while for **2** the coordination geometry about each *exo*-cyclic tin atom, Sn(1), is completed by one bridging and one monodentate carboxylate ligand. A pentacyclic and a tricyclic ring system with the central unit of $Sn_2O_2$ are exhibited by **1** and **2**, respectively. The coordination number around each tin is five for **2** and five and six around Sn(1) and Sn(2), respectively, for **1**. Analysis of the shape determining angles for **2,** using the approach of Reedijk and coworkers [12], yields $\tau$ $((\alpha-\beta)/60)$ values of 0.40 and 0.38 for Sn(1) and Sn(2), respectively ($\tau=0.0$ and 1.0 for SPY and TBPY geometries, respectively). The metal coordination geometry is therefore described as distorted square pyramidal with the O(1) atom occupying the apical positions for both Sn(1) and Sn(2). The donor O(1) is chosen as apex by the simple criterion that it should not be one of the oxygens which defines either of the two largest L–Sn–L angles, $\alpha$ and $\beta$ [12]. Distortions from the ideal geometries may be related to the close approach (2.800(3) Å) of the O(4a) atom to Sn(2), and of the O(5) atom to Sn(1) (2.727(3) Å) (symmetry operation (i): $1-x$, $-y$, $-z$). These distances are long for primary Sn–O bonding, but are similar to an intermolecular approach in the $Bu_2Sn(IV)$ complex of piroxicam [9e] and other complexes [13] and therefore represent a type of secondary interaction. Analysis of the shape determining angles for Sn(1) in **1** gives a $\tau$ value of 0.80. The metal coordination geometry is therefore described as distorted trigonal bipyramidal with the O(2) and O(5a) atoms occupying the axial positions and O(1), C(1) and C(2), the equatorial positions.

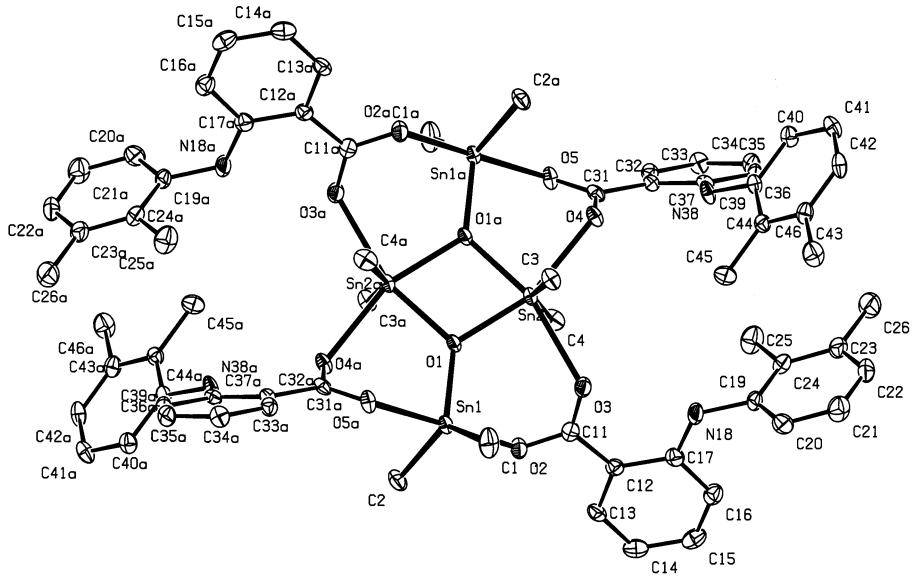

Fig. 1. Perspective view of $[Me_2SnLOLSnMe_2]_2$ (**1**) showing the atomic numbering scheme.

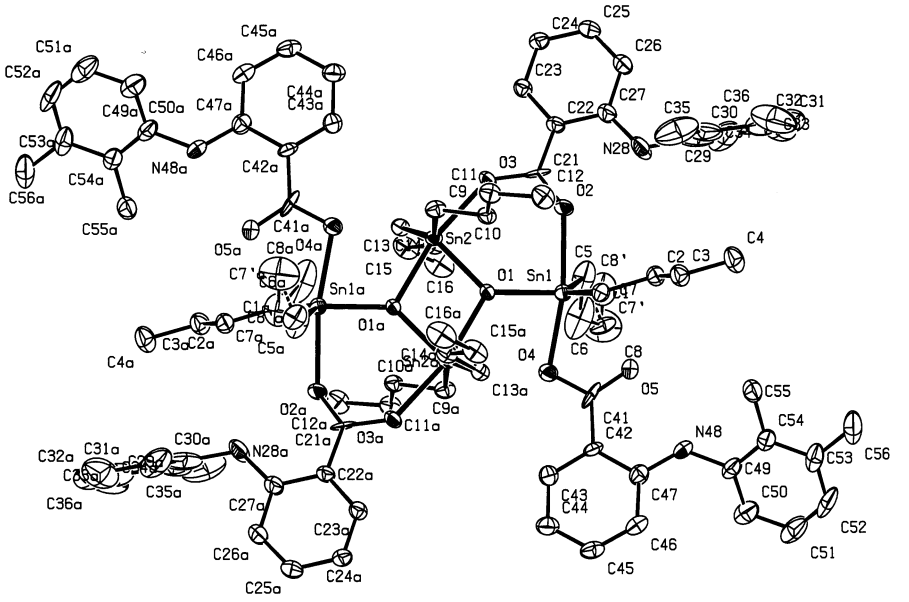

Fig. 2. Perspective view of $[Bu_2SnLOLSnBu_2]_2$ (**2**) showing the atomic numbering scheme.

For **1**, the Sn–O bond distances involving the bridging carboxylate ligands differ by 0.3254 and 0.2312 Å indicating asymmetrical bridges; the variations in the C–O bond distances are much less and suggest charge delocalization over the carboxylato group COO. For **2**, the Sn(1)–O(2), Sn(2)–O(3) bond distances involving the bridging carboxylate ligand, 2.290(3) and 2.227(3) Å, respectively, differ by only 0.063 Å indicating a nearly symmetrical bridge; this is supported by both distances being longer than the Sn(1)–O(4) bond distance, 2.171(3) Å, formed by the monodentate carboxylato ligand. The monodentate carboxylato has a difference of 0.112 between its C–O bonds while for the bidentate carboxylato this difference is only 0.034. The different modes of bonding of the acetates, i.e. bridging or hanging, are thus easily differentiated by the relevant bond lengths.

The phenyl rings are planar. The dihedral angles between the planes of the phenyl rings in **1** are 88.48(16) and 48.13(16)° for the bidentate ligands bridging the two centers Sn(1)–Sn(2) and Sn(1)–Sn(2a), respectively. The dihedral angles between the planes of the phenyl rings for **2** are 73.8(4) and 47.0(3)°, respectively, for the bidentate bridging and the monodentate ligands. The aminobenzoate portion of each carboxylato ligand is effectively planar which presumably facil-

itates the formation of intramolecular N(28)–H···O(2) and N(48)–H···O(5) interactions of 2.643(9) and 2.632(5) Å, respectively. By contrast, significant twists between the aromatic fragments of bidentate and monodentate ligands are noted.

The crystal structures of **1** and **2** show ring stacking interactions. For **1**, the phenyl ring C(39)–C(46) of the tetramer 'faces' the corresponding phenyl ring of an adjacent tetramer at a distance of 3.587 Å showing significant $\pi \rightarrow \pi$ stacking interactions. For **2**, the phenyl ring C(22)–C(27) 'faces' the phenyl ring C(42)–C(47) at a distance of 3.785 Å. Further, C–H $\rightarrow \pi$ interactions and intramolecular hydrogen bonds stabilize the two structures. The polar imino hydrogen atoms on N(18), N(38) and N(28), N(48) for **1** and **2**, respectively, participate in a bifurcated intramolecular hydrogen bond system, as shown in Table 3. In this case complexes **1** and **2** are self-assembled via C–H $\rightarrow \pi$ and $\pi \rightarrow \pi$ stacking interactions and a different packing arrangement from bis(2-[(2,6-dichlorophenyl)amino]-phenyl]acetate) oxide results [9f]. The overall geometry found in the structures of **1** and **2,** allowing for differences in chemistry, are remarkably similar to compounds with the general formula $[R_2(R'CO_2)SnOSn(O_2CR')R_2]_2$ [14]. Views of the crystal packing along the $\alpha$ axes for **1** and **2** are shown in Figs. 3 and 4, respectively.

Table 2
Bond lengths (Å) and bond angles (°) for **1** and **2** [a]

| **1** | | **2** | |
|---|---|---|---|
| *Bond lengths* | | | |
| Sn(1)–O(1) | 2.0059(18) | Sn(1)–O(1) | 2.027(3) |
| Sn(1)–C(1) | 2.107(3) | Sn(1)–C(5) | 2.123(5) |
| Sn(1)–C(2) | 2.108(3) | Sn(1)–C(1) | 2.125(4) |
| Sn(1)–O(2) | 2.1656(19) | Sn(1)–O(4) | 2.171(3) |
| Sn(1)–O(5$^{i}$) | 2.1911(19) | Sn(1)–O(2) | 2.290(3) |
| Sn(2)–O(1$^{i}$) | 2.0935(19) | Sn(2)–O(1) | 2.034(3) |
| Sn(2)–C(3) | 2.102(3) | Sn(2)–C(13) | 2.117(4) |
| Sn(2)–O(1) | 2.1055(18) | Sn(2)–C(9) | 2.122(4) |
| Sn(2)–C(4) | 2.107(3) | Sn(2)–O(1$^{i}$) | 2.173(3) |
| Sn(2)–O(4) | 2.4223(18) | Sn(2)–O(3) | 2.227(3) |
| Sn(2)–O(3) | 2.491(2) | O(1)–Sn(2$^{i}$) | 2.173(3) |
| O(1)–Sn(2$^{i}$) | 2.0935(19) | O(2)–C(21) | 1.233(5) |
| O(2)–C(11) | 1.275(3) | O(3)–C(21) | 1.345(5) |
| O(3)–C(11) | 1.265(3) | O(4)–C(41) | 1.301(5) |
| O(4)–C(31) | 1.268(3) | O(5)–C(41) | 1.267(6) |
| O(5)–C(31) | 1.271(3) | | |
| *Bond angles* | | | |
| O(1)–Sn(1)–C(1) | 114.16(14) | O(1)–Sn(1)–C(5) | 110.91(18) |
| O(1)–Sn(1)–C(2) | 116.39(11) | O(1)–Sn(1)–C(1) | 112.51(15) |
| C(1)–Sn(1)–C(2) | 129.43(16) | C(5)–Sn(1)–C(1) | 134.9(2) |
| O(1)–Sn(1)–O(2) | 89.31(7) | O(1)–Sn(1)–O(4) | 80.33(11) |
| C(1)–Sn(1)–O(2) | 93.84(13) | C(5)–Sn(1)–O(4) | 102.2(2) |
| C(2)–Sn(1)–O(2) | 85.44(11) | C(1)–Sn(1)–O(4) | 96.52(14) |
| O(1)–Sn(1)–O(5$^{i}$) | 90.52(7) | O(1)–Sn(1)–O(2) | 89.38(11) |
| C(1)–Sn(1)–O(5$^{i}$) | 89.12(13) | C(5)–Sn(1)–O(2) | 84.3(2) |
| C(2)–Sn(1)–O(5$^{i}$) | 91.80(11) | C(1)–Sn(1)–O(2) | 84.43(15) |
| O(2)–Sn(1)–O(5$^{i}$) | 176.82(7) | O(4)–Sn(1)–O(2) | 169.23(12) |
| O(1$^{i}$)–Sn(2)–C(3) | 101.78(11) | O(1)–Sn(2)–C(13) | 108.38(14) |
| O(1$^{i}$)–Sn(2)–O(1) | 75.95(8) | O(1)–Sn(2)–C(9) | 108.44(14) |
| C(3)–Sn(2)–O(1) | 99.69(10) | C(13)–Sn(2)–C(9) | 142.94(17) |
| O(1$^{i}$)–Sn(2)–C(4) | 101.06(11) | O(1)–Sn(2)–O(1$^{i}$) | 76.18(12) |
| C(3)–Sn(2)–C(4) | 152.08(14) | C(13)–Sn(2)–O(1$^{i}$) | 94.14(13) |
| O(1)–Sn(2)–C(4) | 101.24(11) | C(9)–Sn(2)–O(1$^{i}$) | 98.49(14) |
| O(1$^{i}$)–Sn(2)–O(4) | 84.77(7) | O(1)–Sn(2)–O(3) | 91.12(11) |
| C(3)–Sn(2)–O(4) | 82.06(10) | C(13)–Sn(2)–O(3) | 84.06(14) |
| O(1)–Sn(2)–O(4) | 160.62(7) | C(9)–Sn(2)–O(3) | 91.15(15) |
| C(4)–Sn(2)–O(4) | 84.26(10) | O(1$^{i}$)–Sn(2)–O(3) | 165.95(11) |
| O(1$^{i}$)–Sn(2)–O(3) | 162.81(7) | Sn(1)–O(1)–Sn(2) | 135.39(14) |
| C(3)–Sn(2)–O(3) | 82.10(11) | Sn(1)–O(1)–Sn(2$^{i}$) | 120.31(13) |
| O(1)–Sn(2)–O(3) | 86.90(7) | Sn(2)–O(1)–Sn(2$^{i}$) | 103.82(12) |
| C(4)–Sn(2)–O(3) | 80.81(11) | C(21)–O(2)–Sn(1) | 134.1(3) |
| O(4)–Sn(2)–O(3) | 112.41(6) | C(21)–O(3)–Sn(2) | 134.9(2) |
| Sn(1)–O(1)–Sn(2$^{i}$) | 127.89(9) | C(41)–O(4)–Sn(1) | 107.4(3) |
| Sn(1)–O(1)–Sn(2) | 127.86(9) | C(2)–C(1)–Sn(1) | 115.1(3) |
| Sn(2$^{i}$)–O(1)–Sn(2) | 104.05(8) | | |
| C(11)–O(2)–Sn(1) | 126.46(18) | | |
| C(11)–O(3)–Sn(2) | 118.76(18) | | |
| C(31)–O(4)–Sn(2) | 118.83(17) | | |
| C(31)–O(5)–Sn(1$^{i}$) | 120.19(17) | | |

[a] Symmetry operation (i) $-x$, $-y$, $1-z$.

### 3.2. Spectroscopy

#### 3.2.1. Infrared spectroscopy

The most prominent absorptions are shown in Table 4. Compounds **1** and **2** gave bands at $\sim$3340 and 3290 $cm^{-1}$ attributable to intramolecular hydrogen bonds NH···O. The $\nu_{as}$(COO) and $\nu_{sym}$(COO) bands appear at $\sim$1610–1500 and $\sim$1450–1260 $cm^{-1}$, respectively. The difference, $\Delta$ $[\nu_{as}(COO) - \nu_{sym}(COO)]$ between these frequencies for **1** is close to that found for bridging bidentate carboxylato groups (142 and 126 $cm^{-1}$) and for **2** is close to that found for monodentate (313 $cm^{-1}$) and bridging bidentate carboxylato groups (123 $cm^{-1}$) [4,15]. This is totally consistent with the X-ray structures. Two bands at 490–470 and 430–420 $cm^{-1}$, for each of **1** and **2**, are assigned to $\nu_{as,sym}(SnO)_2$, indicating nonlinear O–Sn–O moieties, while the bands at 250–200 $cm^{-1}$ are assigned to the tin–oxygen (COO) stretching modes [4,14].

#### 3.2.2. Mössbauer spectroscopy

The spectra present slightly asymmetrical quadrupole split doublets, whose parameters are typical of diorganotin complexes [7b]. The linewidths were narrow enough (around 0.8 mm $s^{-1}$) to consider the existence of a single tin site and the parameters pointed to a severely distorted penta-coordinated site. This was acceptable for compound **2**, $\delta$, 1.47; $\Delta E_Q$, 3.27 mm $s^{-1}$, because of the agreement with the crystal structure. On the contrary, this solution is unacceptable for compound **1**, so a fitting of the data to two doublets with the same area was attempted, $\delta$, 1.47 and 1.27; $\Delta E_Q$, 3.43 and 3.12 mm $s^{-1}$. The new solution gives a small improvement in the quality of fit and parameters reasonable for distorted penta- and hexa-coordinated tin

Table 3
Distances (Å) and angles (°) of C–H–π, π–π interactions and intramolecular hydrogen bonds for **1** and **2**

| C–H–π, π–π interactions and intramolecular hydrogen bonds for | | | | | | | | | | | |
|---|---|---|---|---|---|---|---|---|---|---|---|
| **1** | | | | | | **2** | | | | | |
| C–H(I)→Cg(J) | | | H···Cg | C···Cg | ∠C–H···Cg | C–H(I)→Cg(J) | | | H···Cg | C···Cg | ∠C–H–Cg |
| C(15)–H(15)→Cg(7)[I] | | | 2.99 | 3.556 | 121 | C(8)–H(8B)→Cg(4)[iii] | | | 3.07 | 3.851 | 138 |
| | | | | | | C(10)–H(10B)→Cg(1)[iv] | | | 3.23 | 3.597 | 105 |
| | | | | | | C(11)–H(11B)→Cg(3)[v] | | | 3.25 | 3.945 | 130 |
| | | | | | | C(14)–H(14A)→Cg(1)[iv] | | | 3.00 | 3.475 | 112 |
| | | | | | | C(30)–H(30)→Cg(6)[i] | | | 3.14 | 3.825 | 131 |
| | | | | | | C(51)–H(51)→Cg(4)[vi] | | | 2.81 | 3.660 | 153 |
| | | | | | | C(55)–H(55C)→Cg(6)[vi] | | | 2.86 | 3.798 | 167 |
| Cg(I)→Cg(J) [a] | | Cg–Cg [b] | β [c] | CgI-Perp [d] | CgJ-Perp[e] | Cg(I)→Cg(J) [a] | | Cg–Cg [b] | β [c] | CgI-Perp [d] | CgJ-Perp [e] |
| Cg(8)→Cg(8)[ii] | | 3.587 | 14.40 | 3.475 | 3.475 | Cg(3)→Cg(5)[i] | | 3.785 | 25.19 | 3.562 | 3.425 |
| | | | | | | Cg(5)→Cg(3)[vii] | | 3.785 | 19.74 | 3.425 | 3.562 |
| D | H | A [f] | D···A | H···A | ∠D–H···A | D | H | A [f] | D···A | H···A | ∠D–H···A |
| N(18) | H(18) | O(3) | 2.712(4) | 2.07(3) | 141(3) | N(28) | H(28) | O(2) | 2.643(9) | 1.97 | 132 |
| N(38) | H(38) | O(4) | 2.687(3) | 2.05(3) | 137(3) | N(48) | H(48) | O(5) | 2.632(5) | 1.99 | 141 |
| C(33) | H(33) | O(5) | 2.741(4) | 2.42(3) | 102(2) | C(23) | H(23) | O(3) | 2.730(6) | 2.40 | 101 |
| | | | | | | C(43) | H(43) | O(4) | 2.775(6) | 2.45 | 101 |

[a] Cg(7) and Cg(8) are referred to the centroids C(32)–C(38) and C(39)–C(44) for **1**, Cg(1), Cg(3), Cg(4), Cg(5) and Cg(6) are referred to the centroids Sn(2)–O(1)–Sn(2a)–O(1a), C(22)–C(27), C(29)–C(34), C(42)–C(47) and C(49)–C(54) for **2**.

[b] Cg–Cg is the distance between ring centroids; symmetry transformations: (i) $x, -1+y, z$; (ii) $-x, 3-y, -z$; (iii) $-1+x, y, z$; (iv) $1-x, -y, -z$; (v) $2-x, -y, -z$; (vi) $2-x, 1-y, 1-z$; (vii) $x, 1+y, z$.

[c] $\beta$ is the angle Cg(I)→Cg(J) or Cg(i)→Me vector and normal to plane I (°).

[d] CgI-Perp is the perpendicular distance of Cg(I) on ring J.

[e] CgJ-Perp is the perpendicular distance of Cg(J) on ring I.

[f] D is donor and A is acceptor.

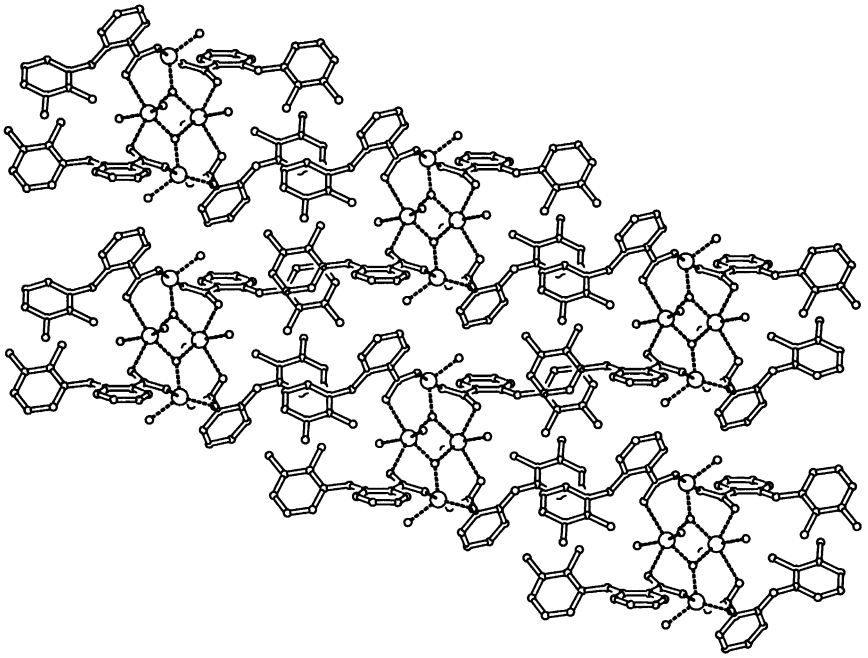

Fig. 3. Packing diagram of the complex of $[Me_2SnLOLSnMe_2]_2$ (**1**) viewed along the $\alpha$ axis.

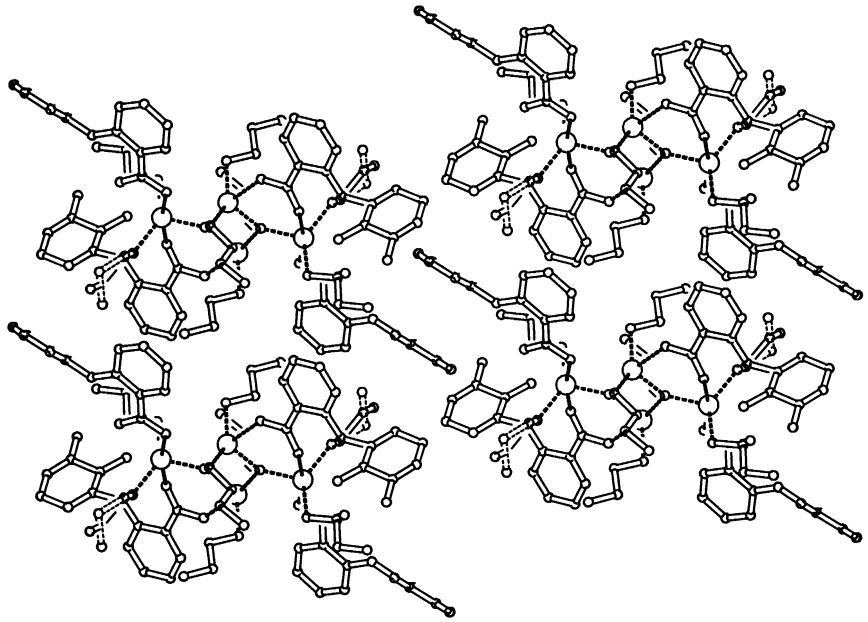

Fig. 4. Packing diagram of the complex of $[Bu_2SnLOLSnBu_2]_2$ (**2**) viewed along the $\alpha$ axis.

Table 4
Selected IR absorption bands ($cm^{-1}$) of organotin(IV) complexes

| No. | $\nu$(NH) | $\nu_{as}$(COO) | $\nu_{sym}$(COO) | $\Delta$ | $\nu(SnO)_2$ | $\nu$(SnC) | $\nu$(SnO) | $\delta$(SnO) |
|---|---|---|---|---|---|---|---|---|
| NaL | 3291s | 1580s | 1390s | 180 | | | | |
| **1** | 3310m | 1615s | 1473s | 142 | 473ms | 550mw | 246m | 174mw |
| | 3248s | 1580s | 1454ms | 126 | 426vs | 522m | 219m | 147mw |
| | | | | | | 505vs | | |
| **2** | 3325s | 1615s | 1272s | 313 | 479ms | 555mw | 237mw | 185mw |
| | 3254s | 1579s | 1456 | 123 | 428s | 534m | 212mw | 155mw |
| | | | | | | 507m | | |

Table 5
$^{1}H$- and $^{13}C$-NMR data

| | COOH | NH | H3 | H4 | H5 | H6 | H4′ | H5′ | H6′ | 2′-$CH_3$; 3′-$CH_3$ |
|---|---|---|---|---|---|---|---|---|---|---|
| Mef [a] | [b] | 9.11s | 8.03d | 6.69dd | 7.28t | 6.69dd | 7.10m [c] | 7.10m | 7.10m | 2.18s/2.34s |
| Mef [d] | 13.12 | 9.52s | 7.94d | 6.71dd | 7.32t | 6.71dd | 7.08m | 7.08m | 7.08m | 2.13s/230s |
| **1** [a] | $Me_2Sn$ 0.96s/1.05s 1.55s/1.55s | 9.35br | 8.00br | 6.99d | 7.10d | 6.79d | 7.18m | 7.18m | 7.18m | 2.17s/2.32 |
| **1** [a] | $Me_2Sn$ 0.75t/0.85t 0.85t/1.23m | 9.77br | 8.26/8.30br | 6.96d/6.11d | 7.21t/7.89 | 6.75d | 7.10m | 7.10m | 7.10m | 2.08s/2.50s |
| 2 [a] | $Bu_2Sn$ Hδ: 0.90, Hγ: 1.25, Hα, β: 1.54 | 9.45 9.19 | 8.10d | 6.84d | 7.17t | 6.75d | 7.11m | 7.11m | 7.11m | 2.17s/2.50s |

| | COOH | C1 | C2 | C3 | C4 | C5 | C6 | C1′ | C2′ | C3′ | C4′ | C5′ | C6′ | 2′-$CH_3$; 3′-$CH_3$ |
|---|---|---|---|---|---|---|---|---|---|---|---|---|---|---|
| Mef. [a,e] | 173.05 | 150.3 | 109.2 | 132.4 | 116.1 | 135.2 | 113.7 | 138.4 | 132.9 | 138.8 | 123.7 | 126.0 | 127.2 | 20.7/14.3 |
| **1** [a] | COOH 177.0 $Me_2Sn$: 5.0/8.5 | 149.8 | 110.9 | 133.2 | 116.2 | 134.8 | 113.5 | 138.2 | 132.2 | 138.2 | 122.6 | 125.7 | 126.2 | 20.5/14.0 |
| **2** [a] | $Bu_2Sn$ Cδ: 12.5, Cγ: 26.9, Cβ: 27.7, Cα:25.6 | 149.8 | 113.3 | 133.4 | 115.8 | 135.0 | 113.3 | 137.4 | 132.6 | 139.3 | 122.5 | 125.7 | 126.2 | 20.6/13.9 |

[a] Spectrum recorded in $CDCl_3$.
[b] Carboxyl proton exchanged in $CDCl_3$.
[c] These resonances formed a multiplet.
[d] Spectrum recorded in DMSO-$d_6$.
[e] Ref. [15].

sites. However, both solutions are acceptable from a Mössbauer point of view, thereby demonstrating that the molecular structures cannot be derived from Mössbauer data in isolation.

*3.2.3. NMR spectra*

The $^{1}$H- and $^{13}$C-NMR data for mefenamic acid, structure 1 and the complexes are summarized in Table 5. These results, together with the published data on mefenamic acid [16] allowed complete assignment of all signals in the spectra of both the mefenamic acid and organotin complexes. The downfield chemical shift for HN in mefenamic acid indicates that this proton is involved in hydrogen bonding. The crystal structure of mefenamic acid suggests the presence of hydrogen-bonded dimers linked by two intermolecular O···H–O hydrogen bonds and an intramolecular hydrogen bond between the HN group and the carbonyl group of the carboxyl acid [6a]. The existence of the HN resonance in the $^{1}$H-NMR spectra indicates that the nitrogen atoms remain protonated in **1** and **2**. In the $^{1}$H-NMR spectrum of **1**, three singlets appear in the region of the tin-bound methyl groups, in the case of the multiple signal emerging at 1.55 ppm, two methyl groups are present. For **1**, the appearance of two resonances for each of H(3), H(4) and H(5), shows the existence of two inequivalent ligands in DMSO-$d_6$ solution. Deshielding of protons H(3) and H(4) is observed in complexes **1** and **2**, which should be related to the electrophilicity of the tin. A σ-charge donation from the $COO^{-}$ donor to the tin center removes electron density from the ligand and produces this deshielding which will attenuate at positions remote from the metal. All shifts are downfield except for that due to H(5) which is shifted upfield. The upfield shift observed for H(5) and its corresponding carbon atom C5, *para* to the tin center, could be due to the flow of charge from the tin into the aromatic ring [18]. Involvement of the carboxyl group in bonding to Sn is confirmed by the resonances ascribed to C2 and C3, which exhibit the greatest shifts upon coordination. The remaining resonances due to the aromatic carbon atoms do not shift significantly on binding to Sn. No resonance attributable to the carboxyl C nucleus was found for **2**, behavior that has been noted previously for related systems [4]. In the $^{13}$C-NMR spectra, the greatest downfield shift is exhibited by the carbonyl C (4.0 ppm) for **2**, while the C3 atom shifts downfield by 0.8–1.0 ppm. The C5 resonance, by contrast, shifts upfield. Three resonances attributed to the tin-bound methyl carbons are found, a result that is consistent with the presence of a dimer in solution by analogy with related compounds [4,17]. Application of the Lockhart–Manders equation [19] to **1** predicted, in $CDCl_3$ solution, C–Sn–C angles of 133 (two values), 118 and 137°, and in $(CD_3)SO$ solution corresponding values of 132 (two angles), 114 and 159°.

## 4. Supplementary material

Crystallographic data for the structural analysis have been deposited with the Cambridge Crystallographic Data Centre, CCDC nos. 159477 and 159478 for compounds **1** and **2**, respectively. Copies of this information may be obtained free of charge from The Director, CCDC, 12 Union Road, Cambridge CB2 1EZ, UK (Fax: +44-1223-336033; e-mail: deposit@ccdc.cam.ac.uk or www: http://www.ccdc.cam.ac.uk.

## Acknowledgements

D.K.D. thanks VIANNEX A.E. for the generous gift of mefenamic acid. This work was supported by the EPEAEK Program 'Bioinorganic Chemistry', Director Professor N. Hadjiliadis and by the Ministry of Development General Secretariat for Research and Technology (project no AP 17975 to D.K.D. and U.R.).

## References

[1] (a) P.A. Insel, Goodman and Gilman's The Pharmacological Basis of Therapeutics, McGraw-Hill, NewYork, 1996 (chap. 27); (b) J.E.F. Reynolds, K. Parfitt, A.V. Parsons, S.C. Sweetman, Martindale, The Extra Pharmacopoeia, 30th ed., The Pharmaceutical Press, London, 1993, p. 15; (c) W.E.M. Lands, A.M. Hanel, Inhibitors and activators of prostaglandin biosynthesis, in: C. Pace-Asciak, E. Granstrom (Eds.), Prostaglandins and Related Substances, Elsevier Science Publishers, Amsterdam, 1983, pp. 203–223.

[2] B.A. Thicher, T.T. Korbut, K. Menon, S.A. Holden, G. Ara, Cancer Chemother. Pharmacol. 33 (1994) 515.

[3] C.P. Duffy, C.J. Elliott, R.A. O'Connor, M.M. Heenan, S. Coyle, I.M. Cleary, K. Kavanagh, S. Verhaegen, C.M. O'Loughlin, R. Nic Amhlaoibh, M. Clynes, Eur. J. Cancer 34 (1998) 1250.

[4] (a) D. Kovala-Demertzi, N. Kourkoumelis, A. Koutsodimou, A. Moukarika, E. Horn, E.R.T. Tiekink, J. Organomet. Chem. 620 (2001) 194; (b) N. Kourkoumelis, PhD thesis, University of Ioannina, Ioannina, 2000.

[5] (a) H. Bojarowicz, Z. Kokot, A. Surdykowski, J. Pharm. Biomed. Anal. 15 (1996) 339; (b) A. Topacli, S. Ide, J. Pharm. Biomed. Anal. 21 (1999) 975.

[6] (a) V. Dhanaraj, M. Vijayan, Acta Crystallogr. Sect. B 44 (1988) 406; (b) G. Facchin, M.H. Torre, E.J. Baran, Z. Naturforsch. Teil B 53 (1998) 871.

[7] (a) A.G. Davies, Organotin Chemistry, VCH, Weinheim, 1997; (b) in: P.J. Smith (Ed.), Chemistry of Tin, 2nd ed., Blackie Academic and Professional, London, 1998.

[8] (a) M. Gielen, Coord. Chem. Rev. 15 (1996) 41; (b) S.J. Blunden, P.A. Cusack, R. Hill, Industrial Uses of Tin Chemicals, Royal Society of Chemistry, London, 1985; (c) A.J. Crowe, in: M. Gielen (Ed.), Metal-based Antitumour Drugs, vol. 1, Freund, London, 1989.

[9] (a) P. Tauridou, U. Russo, G. Valle, D. Kovala-Demertzi, J. Organomet. Chem. 44 (1993) C16;

(b) D. Kovala-Demertzi, P. Tauridou, A. Moukarika, J.M. Tsangaris, C.P. Raptopoulou, A. Terzis, J. Chem. Soc. Dalton Trans. (1995) 123;
(c) D. Kovala-Demertzi, P. Tauridou, U. Russo, M. Gielen, Inorg. Chim. Acta 239 (1995) 177;
(d) N. Kourkoumelis, A. Hatzidimitriou, D. Kovala-Demertzi, J. Organomet. Chem. 514 (1996) 163;
(e) S.K. Hadjikakou, M.A. Demertzis, J.R. Miller, D. Kovala-Demertzi, J. Chem. Soc. Dalton Trans. (1999) 663;
(f) N. Kourkoumelis, D. Kovala-Demertzi, E. Tiekink, Z. Crystallogr. 214 (1999) 758.

[10] (a) D. Kovala-Demertzi, D. Mentzafos, A. Terzis, Polyhedron 11 (1993) 1361;
(b) D. Kovala-Demertzi, A. Theodorou, M.A. Demertzis, C. Raptopoulou, A. Terzis, J. Inorg. Biochem. 65 (1997) 151;
(c) D. Kovala-Demertzi, S.K. Hadjikakou, M.A. Demertzis, Y. Deligiannakis, J. Inorg. Biochem. 69 (1998) 223;
(d) M. Konstandinidou, A. Kourounaki, M. Yiangou, L. Hadjipetrou, D. Kovala-Demertzi, S.K. Hadjikakou, M.A. Demertzis, J. Inorg. Biochem. 70 (1998) 63;
(e) A. Theodorou, M.A. Demertzis, D. Kovala-Demertzi, E. Lioliou, A.A. Pantazaki, D.A. Kyriakidis, Biometals 12 (1999) 167.

[11] (a) G.M. Sheldrick, SHELXS97: Program for Solution of Crystal Structures, University of Göttingen, Göttingen, Germany, 1997;
(b) G.M. Sheldrick, SHELXL97: Program for Crystal Structure Refinement, University of Göttingen, Göttingen, Germany.

[12] A. Addison, R.T. Nageswara, J. Reedijk, J. Van Rijn, G.C. Verschoor, J. Chem. Soc. Dalton Trans. (1984) 1349.

[13] (a) K.C. Molloy, T.G. Purcell, K. Quill, I.W. Nowell, J. Organomet. Chem. 267 (1984) 237;
(b) A.R. Forrester, S.J. Garden, R.A. Howie, J.L. Wardell, J. Chem. Soc. Dalton Trans. (1992) 2615.

[14] (a) E.R.T. Tiekink, Appl. Organomet. Chem. 5 (1991) 1;
(b) E.R.T. Tiekink, Trends Organomet. Chem. 1 (1994) 71.

[15] K. Nakamoto, Infrared and Raman Spectra of Inorganic and Coordination Compounds, 4th ed., Wiley, New York, 1986.

[16] S.L.A. Munro, D.J. Craik, Magn. Reson. Chem. 32 (1994) 335.

[17] J.S. Casas, A. Castineiras, M.D. Couce, N. Playá, U. Russo, A. Sánchez, J. Sordo, J.M. Varela, J. Chem. Soc. Dalton Trans. (1998) 1513.

[18] M.A. Demertzis, S.K. Hadjikakou, D Kovala-Demertzi, A. Koutsodimou, M. Kubicki, Helv. Chim. Acta 83 (2000) 2787.

[19] T.P. Lockhart, W.F. Manders, Inorg. Chem. 25 (1986) 892.